ELSEVIER

International Journal of Heat and Fluid Flow 20 (1999) 34–47

International Journal of HEAT AND FLUID FLOW

Wall effects on heat losses from hot-wires

C.F. Lange [1], F. Durst [*], M. Breuer

Institute of Fluid Mechanics, University of Erlangen-Nürnberg, Cauerstr. 4, D-91058 Erlangen, Germany

Received 17 January 1998; accepted 7 July 1998

Abstract

A thorough numerical investigation of the two-dimensional heat transfer and laminar flow around a single circular cylinder was performed. The main interest of this study was the flow configuration of a heated cylinder in the vicinity of a wall under conditions that resemble the flow past a hot-wire anemometry (HWA) probe. A finite volume Navier–Stokes solver enhanced by local block refinement and multigrid acceleration guaranteed highly accurate and efficient computational results. As a reference for the influence of the Reynolds and Prandtl numbers on the drag coefficient C_D and Nusselt number Nu, the limiting case of a cylinder in free stream with a very small temperature loading ($\mathscr{T} = 1.003$) was analyzed first. Calculations were performed in the Re range 10^{-4} to 10^2. All the results agreed well with available analytical/numerical and experimental results. By comparison with the reference results, the influence of the temperature dependence of the fluid properties on C_D and Nu was determined. After these extensive verification predictions a study on the influence of the wall proximity in near-wall HWA measurements was tackled based on two limiting cases, a highly conducting and an insulating wall. The investigation allowed an estimate of the velocity correction needed by HWA data. The results for a highly conducting wall agreed well with available experimental results. A new form of bounded velocity correction was proposed for this case. The results for the case of an insulating wall were unexpected and contradictory to previous experimental observations. A detailed analysis of the numerical solution revealed new aspects of this complex flow situation. Existing experimental results with ''nonconducting'' wall materials were shown to reflect a combination of the extreme situations computed numerically. © 1999 Elsevier Science Inc. All rights reserved.

Notation

C_D	drag coefficient
D	cylinder diameter
Ec	Eckert number
f	vortex shedding frequency
g	gravitational acceleration
Gr	Grashof number
k	thermal conductivity
Nu	Nusselt number
P	pressure
Pr	Prandtl number
$\dot{q}$	specific heat flux
Re	Reynolds number
St	Strouhal number
T	temperature
U_i	Cartesian velocity components
$U_\mathscr{T}$	friction velocity
x_i	Cartesian coordinates
β	coefficient of volumetric thermal expansion
Γ	Euler constant
μ	dynamic viscosity
ν	kinematic viscosity
ρ	fluid density
$\mathscr{T}$	temperature loading
$\mathscr{T}_w$	wall shear stress
Φ	viscous dissipation function

Indices

∞	free stream region
f	at arithmetic mean (film) temperature
meas	measured value
w	at the cylinder wall
$*$	nondimensional quantity
+	in wall coordinates

1. Introduction

Hot-wire anemometry (HWA) is a well developed measuring technique widely used in experimental fluid mechanics to obtain local, time-resolved information on fluid velocity fields. It is an indirect measuring technique, i.e. it requires calibration in a known flow field before it can be applied to fluid flow velocity measurements in laminar and turbulent flows. The heat transfer rate from the wire, used in the measurements, depends on various geometrical and design factors, such as dimensions of the probe, connection of the wire to the supporting prongs and inclination of the probe to the flow velocity (see Fig. 1).

* Corresponding author. E-mail: durst@lstm.uni-erlangen.de

[1] Present address: Department of Mech. Engineering, University of Alberta, Edmonton, AB, Canada T6G 2G8.

0142-727X/99/$ – see front matter © 1999 Elsevier Science Inc. All rights reserved.
PII: S0142-727X(98)10038-3

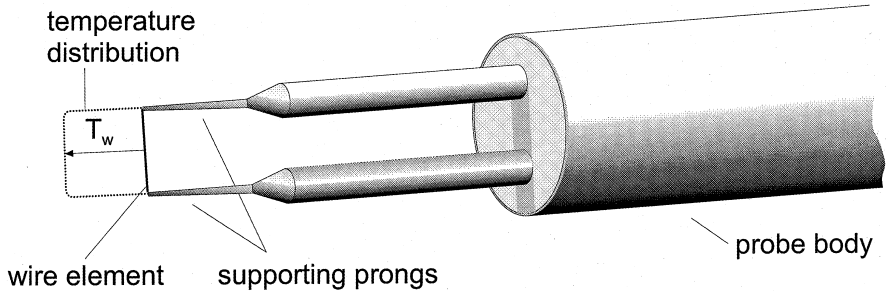

Fig. 1. HWA probe with schematic temperature distribution.

However, if care is taken in the design and measurement procedure to reduce the influence of these factors, e.g. using large length to diameter ratios and assuring orthogonality between wire and velocity directions, the relationship between velocity and heat transfer rate reduces in practice to a problem of two-dimensional flow around a heated cylinder. Fig. 1 shows schematically the geometry and temperature distribution on the wire element of a probe. Hot-wire probes are usually optimized to reduce the influence of the prongs on the temperature distribution along the wire, thus maximizing the region where two-dimensional effects prevail. The reduced two-dimensional problem is still complex. The heat transfer rate is influenced not only by the flow velocity, as one might wish for an ideal probe, but also by fluid properties, such as density, viscosity, Prandtl number etc., and by boundary conditions, such as the temperature difference between wire and fluid.

Wires of typical HWA probes have a diameter of 5μm and temperatures of 150–300°C. The aspect ratio (length-to-diameter ratio) is usually $\geqslant 200$. Wire diameters can range from 0.6 to 60 μm, depending on the fluid and the flow to be measured. Smaller wires (0.6 μm) are used for boundary layer measurements in air and are sometimes heated only 50°C above the air temperature. Considering the described conditions and typical wind tunnel velocities of 5–30 m/s, the Reynolds number of the flow around a cylindrical wire element of an HWA probe ranges between about 0.1 and 100.

The correlation between the flow velocity and the heat transfer rate has been approached mainly empirically and the form of the calibration equations was derived from a large number of experiments (see, e.g., Bruun, 1995). However, many details about the heat transfer process from the wire and the influence of various factors, such as the variation of the fluid properties with temperature or the effect of viscous heating, demand a more accurate analysis. Another factor that may influence heavily the heat transfer from the wire is the proximity of an obstacle or a wall. Although this has been the subject of previous investigations (Bhatia et al., 1982) there still remain some open questions. In the present work, a detailed investigation of the laminar flow around a heated cylinder in free stream and in the vicinity of a wall was aimed at answering some of these questions.

For the computation of the flow around a circular cylinder, a very efficient flow simulation code was employed. The code based on the work of Perić (1985) consists of a finite volume Navier–Stokes solver for block-structured colocated grid arrangements (Perić, 1990; Barcus et al., 1988; Durst et al., 1993; Schäfer et al., 1993). It also incorporates a multigrid scheme for convergence acceleration and is fully parallelized by domain decomposition and a message passing strategy. The use of structured grids is of key importance for the high efficiency of the code, because of the pre-established neighboring relations of the control volumes that allow for the implementation of highly optimized algorithms. At the same time, the grid structure also represented a drawback for the intended investigation. The exigency to continue each grid line up to the boundary caused the extension of a fine grid resolution over the whole domain, even when only part of the domain needed to be refined. This condition resulted in an excess of control volumes and consequently of memory and computing time requirements. A local grid refinement scheme was developed and implemented in order to overcome this disadvantage.

In the case of flow around an immersed body, such as the cylinder in the present investigation, the main region of interest for the computation is usually the vicinity of the body and the wake region behind it. In spite of this, in previous studies (Lange, 1997; Lange et al., 1998) it was shown that the computational domain has to be extended to a certain, in some cases extremely large, distance from the body. This domain extension is needed so that the boundary conditions at the outer border do not disturb the flow solution in the just described region of interest. However, to obtain a solution with a similar level of accuracy over the whole domain it is not necessary to discretize the domain homogeneously. In the vicinity of the body the occurrence of high velocity gradients requires very fine grids. In the wake region moderately fine grids are needed, whereas at larger distances of the body coarser grids may be employed. Hence the flow around a cylinder is a typical problem where local refinement of the grid is needed to yield more accurate flow predictions with the available computational resources.

Taking a specially developed computer code, flow and heat transfer predictions were carried out to obtain the heat losses from hot-wires located close to a wall. Results are presented in this paper for various wire positions with respect to highly conducting and insulating wall materials. The numerical results are compared with results from measurements and other numerical and analytical studies.

2. Literature survey on hot-wire heat transfer

2.1. Heat transfer in free flows

The laminar, two-dimensional flow around a circular cylinder located in a spatially and time constant velocity field has been of continuous interest to researchers involved in basic fluid mechanics. Almost every standard textbook on fluid dynamics describes the different flow structures and the resultant change of the drag coefficient as a function of the Reynolds number (see, e.g., Schlichting and Gersten, 1997). However, most experimental studies have investigated the C_D–Re correlation at high Reynolds numbers ($Re > 1000$). There are comparatively few reliable experimental investigations available on the drag of the cylinders for moderate to very low Reynolds numbers ($Re \leqslant 200$). The classical studies covering

this range of Re numbers (see, e.g., Wieselsberger, 1921; Finn, 1953; Tritton, 1959; Jayaweera and Mason, 1965; Nishioka and Sato, 1974) show a relatively large scatter of the results. In these older investigations the discrepancies increase with decreasing Re number, owing to experimental limitations introduced by the accuracy of the force measurements at low values of Re. Only recently have more reliable experimental results become available. Unfortunately, the relatively recent and more accurate results of Huner and Hussey (1977) are restricted, owing to experimental limitations, to low values of Re ranging from 0.2 to 2.6. These experimental limitations stress the importance of the numerical approach in the thorough investigation of the flow around a circular cylinder over the wide range of Re covered in this study (10^{-4} to 10^{2}).

A somewhat different situation exists for the experimental investigation of the heat transfer from a cylinder at low and moderate Reynolds numbers. Mainly motivated by the necessity to correlate the heat loss from the wire probe with the flow velocity in HWA, numerous studies have been carried out on this topic. The early work of King (1914) provided results in terms of the heat transfer coefficient. It was published one year before Nusselt (1915) suggested the use of a nondimensional number, that is nowadays known by his name, to present heat transfer data. Subsequent investigators focused on the correlation of the Nusselt number with the Reynolds number (e.g. Hilpert, 1933; McAdams, 1954; Collis and Williams, 1959; Merker, 1987). As in the case of C_D, the Nu–Re plots of the experimental investigations show a large scatter in the data. This is in part caused by the inappropriate treatment of the variation of fluid properties with temperature. In the range of very low Reynolds numbers ($Re < 0.1$), the scatter in the results is also due to natural convection effects. The influence of buoyancy and also slip effects due to the small size of the wires can hardly be circumvented in experiments. Again, there is an advantage in the analytical and numerical approaches, because of the possibility of isolating the various effects and investigating them separately.

Recently, the von Kármán vortex street, generated in the wake of the cylinder at moderate Reynolds numbers ($Re \gtrsim 46$), has attracted increasing interest. Whereas in the past mainly two-dimensional flow visualizations were reported in the literature, recent flow visualization experiments provided a better understanding of the three-dimensional effects in the wake caused by the cylinder ends. This gave rise to various experimental investigations of this flow regime. Williamson (1996) summarized recent advances on this subject. His review made it clear that there is also a need for more detailed information on the pure two-dimensional vortex shedding mode of cylinder flows, which is difficult to isolate in experiments but can be reliably investigated by numerical simulation.

Analytical investigations of the laminar, two-dimensional flow around a circular cylinder at low Reynolds numbers go back to the early work published by Stokes (1851). He linearized the equations for the flow at very low Reynolds numbers about the vicinity of the cylinder. Stokes found that the resulting boundary value problem has no solution. This is known as the *Stokes paradox*. Many years later, Oseen (1910) explained that this paradox resulted from the neglect of the nonlinear inertia terms, which become dominant far from the cylinder. He suggested that the problem could be avoided by linearizing the flow equations at infinity and thereby partially taking the inertia terms into account. Soon thereafter, Lamb (1911) found a solution of Oseen's equations for a circular cylinder which employed an approximate boundary condition at the surface. It provided a first approximation of the flow around the cylinder and an analytical expression for the drag. Later, Tomotika and Aoi (1951) derived an expansion equation for the drag, based on their extended solution of Oseen's equations.

Proudman and Pearson (1957) and Kaplun (1957) showed that the problem could be solved to any order of the terms by matching two asymptotic expansions which are valid near to and far from the cylinder, the "Stokes" and the "Oseen" expansions, respectively. Further extensions of the method of matched asymptotic expansions and better results in the region of $Re \approx 1$ were presented by Tamada et al. (1983) and Keller and Ward (1996).

The heat transfer from circular cylinders has also been the subject of analytical investigations, but these studies have not been as intensive as those regarding the drag. The pioneering work of Cole and Roshko (1954) on the heat transfer from cylinders in crossflow was based on Oseen's approximation for the flow field, which was applied to the thermal energy equation for small temperature differences (constant fluid properties). They found the first term of an expansion series in $[\ln(\mathrm{Re}\,\mathrm{Pr})]^{-1}$ for the Nusselt number. Wood (1968) extended the work of Cole and Roshko (1954), determining two additional terms in the Oseen expansion of the velocity and temperature fields. Hieber and Gebhart (1968) obtained a similar solution matching two asymptotic expansions of the temperature and employing the flow solution of Kaplun (1957) and Proudman and Pearson (1957). Kassoy (1967) also employed the method of matched asymptotic expansions, but on a more complex formulation, including compressibility effects and variable fluid properties. He investigated successfully the effect of the temperature dependence of the fluid properties on the drag coefficient and on the Nusselt number for low values of Re. His analytical solution was experimentally verified by Aihara et al. (1967).

All the theoretical efforts cited above already faced extreme difficulties in treating flows past a cylinder for $Re \gtrsim 2$. Hence there are at present insufficient analytical results available to add reliable information to the experimental findings on the laminar, two-dimensional flow around circular cylinders at $Re \gtrsim 2$. The situation described readily suggests that numerical investigations are the only means of investigating successfully the flow past circular cylinders over a wide range of Reynolds numbers, where either the experimental or the analytical methods fail to provide accurate information on the flow field and on integral flow properties. This is particularly the case when flows around heated cylinders with larger temperature differences are considered and variable fluid properties need to be taken into account. These observations triggered the work reported in this paper.

The early numerical studies of the flow around circular cylinders used in general a stream function–vorticity formulation of the equations. Thom (1933) presented the first published calculation on the flow past a cylinder at Reynolds numbers of 10 and 20. Later, Kawaguti (1953) integrated the stream function and the vorticity equations for a Reynolds number of 40. These pioneering papers reported computations carried out manually. The latter took, for example, 18 months to perform 10 iterations. In the next decade, the first unsteady calculations of the impulsively started symmetric flow around a circular cylinder (Kawaguti and Jain, 1966; Ingham, 1968) and the first investigations of the effect of the domain size (Keller and Takami, 1966) appeared, together with the use of computers for the calculations. However, the unsteady computations at that time were restricted to time marching of the solution starting from the fluid at rest up to the steady-state solution.

Perhaps the first unsteady computation of the cylinder wake was the work of Hirota and Miyakoda (1965), which demonstrated successfully the development of the von Kármán vortex street at $Re = 100$. Later, Thoman and Szewczyk (1969) computed transient solutions for a wide range of Re from 1 to 10^{5}. In addition to the drag, usually the pressure distribution,

streamlines and vorticity contours were presented for some Reynolds numbers. The number of papers on the numerical computation of the flow past a cylinder grew rapidly with time. The main reason was the attraction of this physical problem, with rather simple geometry, but complicated flow structure. Many newly developed numerical techniques and their variations were tested using the cylinder flow. With few exceptions, such that by Sucker and Brauer (1975), most of the investigations did not really study the physical aspects of the flow, but were merely interested in the validation and demonstration of the abilities of the computer codes employed. With recently increasing interest in the onset of the von Kármán vortex street and its instabilities, many numerical investigations have been carried out on this subject (e.g. Karniadakis and Triantafyllou, 1992; Noack and Eckelmann, 1994; Dušek et al., 1994; Henderson and Barkley, 1996; Barkley and Henderson, 1996; Dauchy et al., 1997). On the other hand, only a few numerical investigations dealing with very small Reynolds numbers (Re < 0.1) are available.

Compared with the isothermal flow past a cylinder, there are remarkably few publications on the numerical solution of the heat transfer from a cylinder in crossflow. The available publications describe the study of pure forced convection, (e.g. Dennis et al., 1968; Sucker and Brauer, 1976), the influence of buoyancy (e.g. Ho et al., 1990; Sundén, 1983; Hatanaka and Kawahara, 1995), or the influence of viscous heating on forced convection (e.g. Sundén, 1992).

2.2. Heat transfer close to a wall

Usually, HWA probes are calibrated in a free stream with controlled velocity and the coefficients of a correlation equation are adjusted for the particular probe. By means of this correlation, the measured values for the heat flux from the wire are converted into precise velocity data. This procedure presupposes that the flow and heat transfer conditions remain similar to the conditions at calibration. This similarity can no longer be assumed in the vicinity of a wall, requiring correction of the measured data.

The need for correction in HWA measurements near walls has been known since the early applications of the technique. In a good review of the literature on this subject, Bhatia et al. (1982) cited two studies that, in the first half of this century, proposed corrections for near-wall HWA measurements. In a later study, which was one of the first to deal with the corrections for constant-temperature HWA probes, Wills (1962) obtained corrections based on the known velocity distribution in a well-defined laminar channel flow. He expected these corrections to be applicable to turbulent boundary layer flows, provided that they had the same friction velocity $U_{\mathscr{T}}$ as in the laminar channel flow used for calibration. The friction velocity is defined as

$$U_{\mathscr{T}} = \sqrt{\frac{\mathscr{T}_w}{\rho}}, \tag{1}$$

where $\mathscr{T}_w$ is the molecular momentum transport term at the wall, also known as wall shear stress. The friction velocity is traditionally employed to normalize the velocity and the distance from the wall in turbulent flows. The resulting nondimensional quantities are, respectively,

$$U^+ = \frac{U}{U_{\mathscr{T}}}, \qquad Y^+ = \frac{yU_{\mathscr{T}}}{\nu}, \tag{2}$$

where U is the velocity component parallel to the wall, y the perpendicular distance from the wall and ν the kinematic viscosity of the fluid. In case of a linear variation of U with y, as in the near-wall part of the laminar boundary layer [2], the following relationship applies

$$U^+ = Y^+. \tag{3}$$

This linear velocity distribution also occurs in the laminar sublayer of a turbulent boundary layer. Based on this, Wills (1962) found his laminar corrections to be too large for application to turbulent flow measurements. He concluded that only half of the laminar correction should be applied, in order to obtain the expected linear velocity distribution in the sublayer. However, no physical explanation could be given for this partial correction.

Later, Oka and Kostić (1972) and Hebbar (1980) obtained corrections by measuring directly turbulent flows in a channel and over a flat plate, respectively. They concluded that their corrections were universal, i.e. were applicable to flows with different values of $U_{\mathscr{T}}$. Hence they expressed their corrections in terms of ΔU^+ and Y^+, the former being defined as

$$\Delta U^+ = \frac{U_{\text{meas}} - U}{U_{\mathscr{T}}}, \tag{4}$$

where U_{meas} is the measured apparent velocity.

More recently, Krishnamoorthy et al. (1985) performed a more complete experimental investigation, considering also the influence of the wire diameter and of the temperature loading on the velocity corrections. They concluded that the correction at a given Y^+ increases with increasing cylinder diameter and temperature loading, hence contesting the universality of corrections based exclusively on the nondimensional wall distance Y^+. Unfortunately, the scatter of their data did not allow a quantitative rule for these additional influences to be established.

In all experimental investigations, the data were very scattered at the closest distances from the wall ($Y^+ \lesssim 1.5$), owing to uncertainties in the determination of the wire position. On the other hand, for $Y^+ \gtrsim 2.5$, again a large scatter was obtained, because of the small values of ΔU^+.

One of the few numerical investigations on this subject is the work of Bhatia et al. (1982). In their study, a very simplified model was considered. The flow field was prescribed in the entire domain as a Couette flow, i.e. $\partial U/\partial y = \text{constant}$, without any influence of the wire. Consequently, only the energy balance equation needed to be solved. The wire was simply treated as a line source and constant fluid properties were used. Their model was based on the assumption that no flow field interference between the wire and the wall would take place for wire positions of $Y^+ \gtrsim 2$. The influence of the wall was assumed to be caused solely by the distortion of the temperature wake of the wire. Two different cases were considered: one of an insulating wall and the other of a highly conducting wall, which was held at ambient temperature.

Bhatia et al. (1982) concluded from their computations that no correction is needed in the case of an insulating wall. Their corrections for the case of a highly conducting wall are larger than the experimentally obtained values for $Y^+ \gtrsim 2.5$, but are among the corrections obtained by Krishnamoorthy et al. (1985) for lower values of Y^+.

In his recent book on HWA, Bruun (1995) concludes that no universal correction procedure has been established so far, because of the various parameters that influence this correction.

[2] Based on the analytical solution of Blasius for the boundary layer equations and on the flat plate measurements of Nikuradse, about one-third of the laminar boundary layer thickness can be considered to have a linear distribution of the velocity with y (see, e.g., Schlichting and Gersten, 1997).

Hence, as the above literature survey shows, the effect of wall proximity in hot-wire anemometric measurements has been widely investigated. Most of these were experimental investigations and suggested corrections for the velocity readings in the vicinity of a wall (e.g. Wills, 1962; Oka and Kostić, 1972; Hebbar, 1980). Krishnamoorthy et al. (1985) considered additional effects, such as the wire diameter and the overheat ratio, in the case of proximity to heat-conducting walls. The distinctive effect of heat-conducting and adiabatic walls was analyzed numerically by Bhatia et al. (1982), who also presented a comprehensive literature survey. They concluded that the wall material has the main influence on the measurement distortions, whereas the velocity correction is negligible for low heat-conducting (adiabatic) walls. However, this conclusion contradicts some experimental results cited by Bruun (1995). A more extensive numerical investigation of the problem is required in order to clarify this discrepancy.

3. Summary of numerical basis

3.1. Governing equations

In the present study, the investigations are restricted to cases where continuum mechanics and incompressibility can be assumed. The governing nondimensional equations for an incompressible two-dimensional flow expressing the conservation of mass, momentum and energy are as follows:

$$\frac{\partial}{\partial x_i^*}(\rho U_i^*) = 0, \tag{5}$$

$$\mathrm{St}\frac{\partial(U_j^*)}{\partial t^*} + U_i^*\frac{\partial(U_j^*)}{\partial x_i^*} = -\frac{\partial P^*}{\partial x_j^*} + \frac{1}{\mathrm{Re}}\frac{\partial}{\partial x_i^*}\left[\mu^*\frac{\partial U_j^*}{\partial x_i^*}\right] + \frac{\mathrm{Gr}}{\mathrm{Re}^2}T^*, \tag{6}$$

$$\mathrm{St}\frac{\partial T^*}{\partial t^*} + U_i^*\frac{\partial T^*}{\partial x_i^*} = \frac{1}{\mathrm{Re}\,\mathrm{Pr}}\frac{\partial}{\partial x_i^*}\left[k^*\frac{\partial T^*}{\partial x_i^*}\right] + \frac{\mathrm{Ec}}{\mathrm{Re}}\Phi^*, \tag{7}$$

where $(i,\ j = 1,2)$, U_i^* are the Cartesian velocity components normalized to the free stream velocity U_∞ and x_i^* are the Cartesian coordinates normalized to the cylinder diameter D, t^* is the time normalized to the vortex shedding frequency f, P^*, the pressure normalized to $\rho_\infty U_\infty^2$, μ^* and k^* are the dynamic viscosity and the thermal conductivity, respectively, normalized to the corresponding value at the free stream temperature, T^* is the temperature normalized to the temperature difference between the cylinder surface and the undisturbed flow $(T_w - T_\infty)$ and Φ^* is the normalized viscous dissipation function, given by

$$\Phi^* = \left(\frac{\partial U_i^*}{\partial x_j^*} + \frac{\partial U_j^*}{\partial x_i^*}\right)\frac{\partial U_i^*}{\partial x_j^*}. \tag{8}$$

The nondimensional parameters relevant to the considered flow problem are as follows:

Strouhal number	$\mathrm{St} = \frac{fD}{U_\infty}$
Prandtl number	$\mathrm{Pr} = \frac{\mu_\infty c_{\mathrm{P}\infty}}{k_\infty}$
Grashof number	$\mathrm{Gr} = \frac{D^3 g\beta\rho_\infty^2(T_w - T_\infty)}{\mu_\infty^2}$
Reynolds number	$\mathrm{Re} = \frac{\rho_\infty U_\infty D}{\mu_\infty}$
Eckert number	$\mathrm{Ec} = \frac{U_\infty^2}{c_{\mathrm{P}\infty}(T_w - T_\infty)}$

where g is the gravitational acceleration, β the coefficient of volumetric thermal expansion, ρ_∞ the density and $c_{\mathrm{P}\infty}$ the specific heat at constant pressure, the last two evaluated at the free stream temperature T_∞.

In the case of small temperature differences between the cylinder and the undisturbed flow, the fluid properties may be treated as constant. Consequently, the nondimensional properties μ^* and k^* are set to unity for this case. Owing to the dimensions and temperatures involved in the present investigation, natural convection and viscous dissipation effects are small. Therefore, the last terms in Eqs. (6) and (7) were neglected. A detailed justification for neglecting these physical effects and for the assumptions of continuum and incompressibility can be found elsewhere (Lange, 1997; Lange et al., 1998).

3.2. Discretization and solution procedure

For the spatial discretization of Eqs. (5)–(7), a finite volume method with a colocated arrangement of the variables was employed, as described by Demirdžić and Perić (1990). Eqs. (6) and (7) were integrated over each control volume (CV), leading to a balance equation for the fluxes through the CV faces and the volumetric sources. Note that in Eqs. (6) and (7) the fluid properties were not treated as being constant. They were calculated as functions of temperature and were updated in each new iteration. The convection and diffusion contributions to the fluxes were evaluated using a central differencing scheme, which for the convective part was implemented using the deferred correction approach proposed by Khosla and Rubin (1974).

For the pressure calculation, a pressure correction equation was used instead of Eq. (5) and was solved iteratively with Eq. (6) following the well-known SIMPLE algorithm. Convergence was achieved when the maximum sum of the normalized absolute residuals in all equations was reduced to $< 10^{-6}$. Details of the discretization and the pressure–velocity coupling can be found elsewhere (Demirdžić and Perić, 1990).

For the time discretization, a slightly modified form of the Crank–Nicolson scheme was applied ensuring a high temporal accuracy (see Lange, 1997). A few steps of the first-order fully implicit Euler scheme were used at the beginning of a new transient computation to prevent the occurrence of small spurious velocity oscillations in the vicinity of the cylinder. In the case of steady-state solutions $(\mathrm{Re} \leqslant 45)$, the stationary forms of Eqs. (6) and (7) were solved instead.

The solver for the linearized systems of equations was based on an incomplete LU decomposition. A nonlinear multigrid scheme was employed for convergence acceleration (see, e.g., Durst et al., 1993; Schäfer et al., 1993). For parallel computations a block structured grid partitioning and a message-passing strategy were used, as described by Durst and Schäfer (1996).

In order to improve the accuracy of the numerical results without a decrease in efficiency and to optimize the utilization of the available computational resources, local grid refinement was employed. For the local refinement procedure, the computational domain was divided into blocks and each block was discretized with a different mesh density. After refinement, each block remained fully structured, hence retaining the very efficient implementation of the code. The combination of high efficiency with high accuracy provided by the local block refinement was essential to the realization of this comprehensive investigation. For more details about the refinement procedure, see the thesis of Lange (1997).

3.3. Verification predictions: cylinder in free stream

In order to verify the employed numerical code, predictions were performed for the flow and heat transfer for a two-dimensional cylinder under free stream conditions in the Re range 10^{-4} to 10^2 (Lange et al., 1998). In this Re range the

laminar flow around a circular cylinder has three regimes: steady flow without separation ($Re \lesssim 5$), steady flow with two symmetric vortices behind the cylinder ($5 \lesssim Re \lesssim 46$) and unsteady flow with vortex shedding ($Re \gtrsim 46$).

Two different types of computational domains and of grids were employed: one for lower and the other for larger values of Re. For all simulations at very low Reynolds numbers ($Re < 1$), the computational domain had to be extremely large and adjusted to the actual value of Re, as has been shown earlier (Lange, 1997; Lange et al., 1998). A domain size up to 10^6 times larger than the cylinder diameter was employed for the smallest value of Re. The region of the flow disturbed by the cylinder at low values of Re is of similar magnitude at its front and rear. Hence a circular domain was chosen. For Reynolds numbers larger than about 5, a pair of standing vortices appear at the rear of the cylinder, demanding a finer discretization of this region. This was taken into account in the refinement process of the grid. The final form of the locally refined grid in the near-cylinder region was chosen after extensive numerical tests (Lange, 1997; Lange et al., 1998) and was then employed as the core region of all numerical grids for stationary computations ($Re \lesssim 46$). At the fifth multigrid level (actual computational grid with about 10^5 grid points) the surface of the cylinder was discretized with a total of 448 CVs.

For the transient flow regime at moderate Reynolds numbers ($Re \gtrsim 46$) the computational domain had to be elongated downstream in order to capture correctly the von Kármán vortex street. On the other hand, the cylinder disturbs a smaller region in the front and lateral directions compared with the other regimes. Therefore, a rectangular domain was adopted for this range of Reynolds numbers, coupling an O-type grid around the cylinder with an H-type grid in the elongated part of the domain. The grid points were concentrated around the cylinder and in the wake region. At the fifth level of the OH-grid (about 10^5 grid points), on which the present results for $Re \gtrsim 46$ were actually computed, a total of 576 CVs were used to discretize the cylinder surface. In all cases no-slip BC for the velocity and a constant value for the temperature were prescribed on the cylinder surface. At the inflow boundary all fluid variables were prescribed (Dirichlet boundary condition), whereas at the outflow zero gradient Neumann boundary conditions were applied.

The investigation was restricted to the case of pure forced convection. The fluid considered was air at an inflow temperature of 20°C. The fluid properties were obtained from the VDI property chart of Verein Deutscher Ingenieure (1991). In the case of larger temperature differences, all properties were treated as temperature dependent and interpolated with a quadratic polynomial function. The cylinder diameter varied between 0.5 μm for the lower and 500 μm for the higher values of Re. The cylinder temperature was assumed to be constant with values between 21°C and 166°C. This corresponds to a range of temperature loadings ($\mathscr{T}$) from 1.003 to 1.5, where $\mathscr{T}$ is defined as

$$\mathscr{T} = \frac{T_w}{T_\infty}, \tag{9}$$

where T_w is the constant cylinder or wire temperature and T_∞ the temperature of the undisturbed flow (in K). The inflow velocity was adjusted in order to give the desired value of Re.

3.3.1. Drag coefficient predictions

One of the most important characteristic quantities of the flow around a cylinder is the nondimensional drag coefficient C_D. In the attached and in the steady recirculating flow regimes, i.e. at $Re \lesssim 46$, the only force acting on the cylinder is the drag in the flow direction, defined as the sum of viscous and pressure forces. In the range of small Reynolds numbers, the drag coefficient varies strongly with Re.

The regime of attached flow is also the range of validity of the existing analytical solutions. A comparison of the present results for the drag coefficient with analytical solutions over the entire range of Reynolds numbers computed is shown in Fig. 2. At the lower end of the range ($Re < 10^{-4}$), only the classical Oseen–Lamb (Oseen, 1910; Lamb, 1911) solution was plotted, since all analytical solutions coincide. The excellent agreement of the numerical results with the analytical solutions is remarkable. At larger values of Re the analytical solutions tend to deviate from the computed curve. The drag coefficient expansion calculated by Tomotika and Aoi (1951) shows a visible discrepancy of about 4% already at $Re \approx 0.1$. The matched asymptotic expansion by Kaplun (1957) gives a solution valid up to $Re \approx 1$. Tamada et al. (1983) improved the solution of Kaplun (1957) by taking the full Navier–Stokes equations in the outer region. A better solution at larger Re was also obtained by Keller and Ward (1996) by computing the sum of all terms of two significant series in the matched asymptotic expansion, namely a power series in $(\ln Re)^{-1}$ and Re times a similar power series in $(\ln Re)^{-1}$.When separation starts at the cylinder and a recirculation region develops behind it at $Re \approx 5$, the contributions of the pressure and viscous forces to the drag become out of balance. Then the pressure force tends to dominate the drag, while the viscous force decreases further. The accuracy of the present computations in this flow regime can only be verified by a comparison with experimental data, shown in Fig. 3. The classical results of Wieselsberger (1921) (in tabular form in Prandtl et al., 1923) and Tritton (1959) show a larger scatter in the data. Nishioka and Sato (1974) obtained a more consistent set of data by measuring the momentum thickness of the cylinder wake. Jayaweera and Mason (1965) used the terminal velocity of freely falling cylinders in a viscous liquid to estimate C_D. Their data seem to overestimate C_D at smaller Re and to underestimate C_D at larger Re, in part because of lack of correction for the finite cylinder length. Huner and Hussey (1977) used the same method, but corrected their data to an infinite flow domain and cylinder length. They obtained the most accurate C_D values in the low Re range. The present results show good agreement with these data.

3.3.2. Nusselt number predictions for constant properties

In many practical problems of heat transfer from cylinders, such as for hot wire anemometers, a correlation between the heat transfer rate and the free stream velocity is desired. The

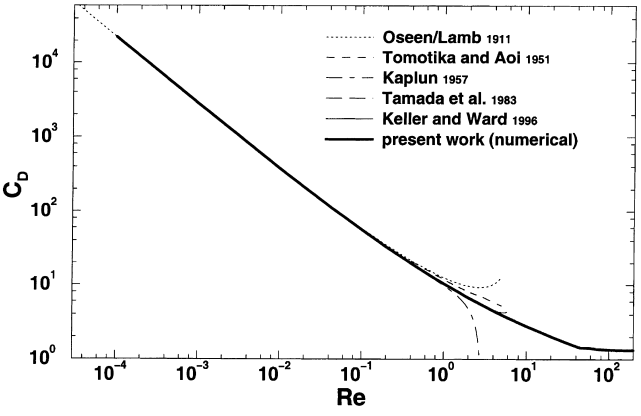

Fig. 2. Drag coefficient: comparison of numerical solution with analytical values over the entire range of Re.

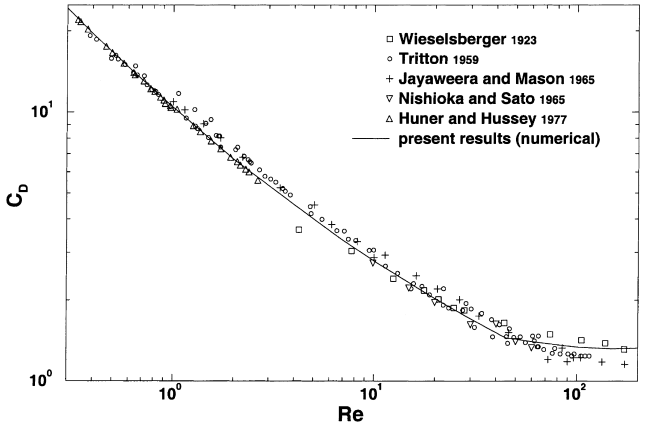

Fig. 3. Drag coefficient: comparison of the present numerical results with experimental values.

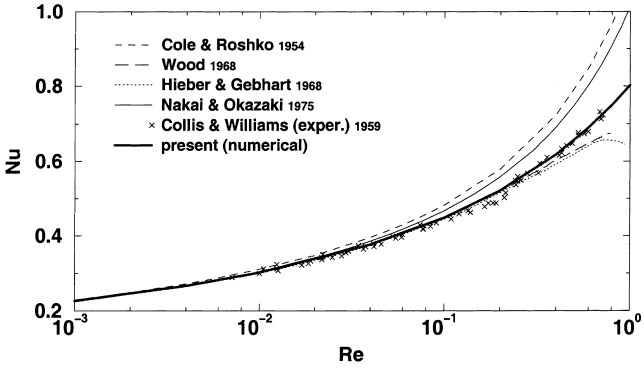

Fig. 4. Nusselt number: comparison of the present numerical results with analytical values.

appropriate nondimensional quantity that addresses the heat transfer by convection is the Nusselt number, Nu. In contrast to other nondimensional parameters such as the Reynolds and Prandtl numbers, Nu is a derived quantity, defined for practical reasons in order to reduce all the heat transfer data to a single correlation. Nusselt (1915) analyzed the heat transfer from cylinders (diameter D) to air in order to find a similarity condition between different flow cases. To establish this similarity, he used a normalized form of the specific heat flux

$$\mathrm{Nu} = \frac{\dot{q}_\mathrm{w}}{\dot{q}_\mathrm{ref}} = \frac{-k_\mathrm{w}\frac{\partial(T-T_\mathrm{w})}{\partial r}\Big|_\mathrm{w}}{k'\frac{(T_\mathrm{w}-T_\infty)}{D}} = \frac{k_\mathrm{w}}{k'}\left.\frac{\partial\left(\frac{T_\mathrm{w}-T}{T_\mathrm{w}-T_\infty}\right)}{\partial\left(\frac{r}{D}\right)}\right|_\mathrm{w}, \tag{10}$$

where $\dot{q}_\mathrm{w}$ is the heat transfer rate per unit area from the cylinder wall to the fluid, $\dot{q}_\mathrm{ref}$ a reference heat flux, k_w the thermal conductivity of the fluid at the cylinder temperature and k' the thermal conductivity at a reference temperature to be defined later. Usually just the mean value of the Nusselt number is needed, namely when no local effect on the cylinder surface is of particular interest. In this case, the value of Nu is averaged over the whole cylinder perimeter. In the following, we consider only the surface averaged value of Nu.

The Nu values are computed first for the case of a very small temperature difference. The cylinder is held at 21°C and the free stream temperature is 20°C. In this case the influence of the temperature dependence of the fluid properties is negligible and the problem of the definition of k' disappears. The Nusselt number depends only on the Reynolds number, since the Prandtl number and all fluid properties remain constant. The main objective of the investigation of this limiting case is to obtain a reference curve for Nu. This means that at any other condition, e.g. at larger temperature differences, the Nu results should coincide with this reference curve, if the normalization is correctly defined.

Based on the Oseen–Lamb (Oseen, 1910; Lamb, 1911) solution for the flow, Cole and Roshko (1954) obtained an analytical expression for the Nusselt number:

$$\mathrm{Nu} = \frac{2}{\ln\frac{8}{\mathrm{Re\,Pr}} - \Gamma}, \tag{11}$$

where $\Gamma \approx 0.5772$ is the Euler constant. Eq. (11) is plotted in Fig. 4 together with other analytical results for the case of air ($\mathrm{Pr} = 0.7148$). Wood (1968) extended Eq. (11) by two terms, whereas Hieber and Gebhart (1968) obtained a solution based on the method of matched asymptotic expansions. Nakai and Okazaki (1975) matched two solutions for the temperature field, one corresponding to pure conduction in the vicinity of the cylinder and the other to a similarity solution for convection in the far field. They obtained the following expression:

$$\mathrm{Nu} = \frac{2}{2/3 + \ln(8/3) - \ln(\mathrm{Re\,Pr})}. \tag{12}$$

Fig. 4 shows that these analytical solutions are valid in the best cases up to $\mathrm{Re} = 0.2$. The experimental data of Collis and Williams (1959) are also shown for comparison.

Fig. 5 shows a comparison with the most consistent experimental values of the Nusselt number available for forced convection in air. These data were corrected to compensate for the influence of the temperature dependence of the fluid properties and therefore are suitable for comparison with the present constant property results. The highly consistent data of Hilpert (1933) were later corrected by Fand and Keswani (1973), using more accurate fluid property values and compensating for the temperature difference in the same way as Collis and Williams (1959). The data of Hatton et al. (1970) corresponding to their smallest cylinder ($D = 0.004$ in.) were discarded, because they are inconsistently larger than other results.

Figs. 4 and 5 show the excellent agreement of the present computations with both analytical (in the range of their validity) and experimental results for the Nusselt number over the complete range of Reynolds numbers computed.

As already mentioned, there are only a few publications on the numerical solution of the present problem. Dennis et al. (1968) discretized the stream function–vorticity equations using series truncation and finite difference methods. They applied the solution of Cole and Roshko (1954) as a boundary condition (Eq. (11)), which probably caused the overestima-

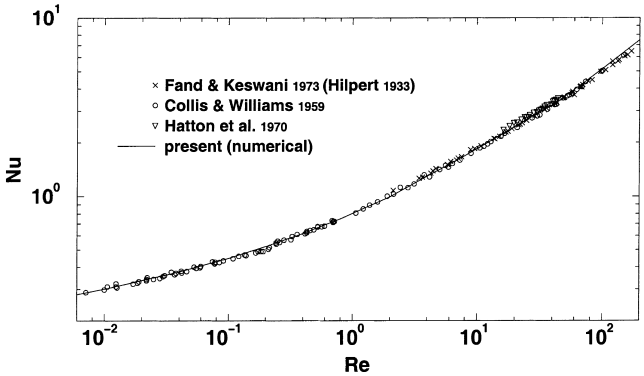

Fig. 5. Nusselt number: comparison of corrected experimental values for cylinders in air with present numerical results.

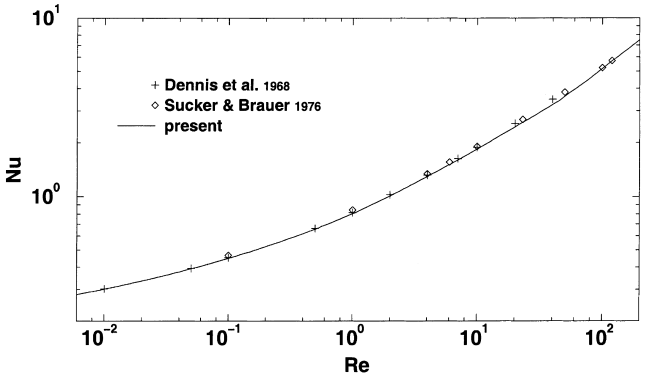

Fig. 6. Nusselt number: comparison of present with other numerical results for cylinders in air.

tion of Nu at $\mathrm{Re} > 10$. Sucker and Brauer (1976) obtained slightly overestimated results in all their computations, except at $\mathrm{Re} = 100$ and 120, where the effect caused by the stationary computation compensated the overestimation. Both numerical results are presented in Fig. 6. Again, the present computations show excellent agreement with other numerical results.

3.3.3. Nusselt number predictions for temperature-dependent properties

The above test case was performed under the condition of constant fluid properties. However, in practical applications of heat transfer from cylinders in crossflow, it is usually essential to consider the influence of the temperature dependence of the fluid properties. The large temperature differences between the cylinder surface and free stream, such as in HWA, do not allow the assumption of constant fluid properties used in the previous section.

We recall that the main goal of the Nusselt number is to serve as a similarity condition to identify the independent parameters governing the convective heat transfer. In the case of constant fluid properties and negligible natural convection and viscous dissipation effects, the Nusselt number depends only on two parameters, namely the Reynolds and Prandtl numbers. Therefore, a plot of the Nusselt number versus a combination of the Reynolds and Prandtl numbers would fit the data of all experiments to a single curve, even with different fluids, satisfying the constant property condition. Unfortunately, there are almost no reliable experiments on forced convection from cylinders with very low temperature differences.

If the temperature differences are not small, the variations of the fluid properties have to be taken into account. As a consequence, Nusselt (1915) showed that the convective heat transfer depends on an additional parameter, namely the temperature loading $\mathscr{T}$, defined in Eq. (9). Consequently, for each value of $\mathscr{T}$, a new Nu curve will be obtained. There have been several attempts to compensate for the temperature dependence of the fluid properties and to circumvent (approximately) the explicit dependence on the temperature loading (Nusselt, 1915; Hilpert, 1933; McAdams, 1954; Schmidt and Wenner, 1941; Douglas and Churchill, 1956; Gersten and Herwig, 1984; Žukauskas and Žiugžda, 1985; Wehle and Brandt, 1982; Herwig and Wickern, 1986; Herwig, 1984). A brief review on this topic is available (Lange, 1997; Lange et al., 1998).

Collis and Williams (1959) published one of the best experimental investigations on the effect of temperature loading and proposed the ratio of the film temperature T_f to the free stream temperature T_∞ as a coefficient to correct Nu_f, the Nusselt number based on properties at the film temperature. They correlated their experimental data by a set of three equations depending on the Reynolds number range considered. More recently, the correction factor of Collis and Williams (1959) was used by Fand and Keswani (1972) to derive a single equation correlating the data of many authors over a very large range of Reynolds numbers ($\mathrm{Re}_\mathrm{f} = 10^{-2}$ to 2×10^5).

A similar equation can be derived to fit the complete set of current results. Applying the correction factor of Collis and Williams (1959) and consistently calculating Re and Nu at the film temperature yields

$$\mathrm{Nu}_\mathrm{f}\left(\frac{T_\mathrm{f}}{T_\infty}\right)^{-0.17} = 0.082\,\mathrm{Re}_\mathrm{f}^{0.5} + 0.734\,\mathrm{Re}_\mathrm{f}^{\chi}, \tag{13}$$

where $\chi = 0.05 + 0.226\,\mathrm{Re}_\mathrm{f}^{0.085}$.

Eq. (13) was verified within the limits $10^{-4} \leqslant \mathrm{Re} \leqslant 2 \cdot 10^2$ and $1.003 \leqslant \mathscr{T} \leqslant 1.5$, but it is expected to be valid also for larger values of $\mathscr{T}$. When the present numerical results were plotted with the Nu correction of Collis and Williams (1959), the curves turned out to be virtually indistinguishable over the whole range of Re numbers computed. Because the corrected curves excellently agree with the results for constant fluid properties, they were not plotted again. For a comparison with experiments Fig. 5 should suffice, since the experimental data had temperature loadings varying between 1.1 and 2.0 and the plotted curve represents all the present results well.

4. Hot-wire heat losses close to a wall

4.1. Computational domain and boundary conditions

For the simulation of an HWA probe under near-wall conditions, a cylinder with usual hot-wire dimensions ($D = 5$ μm) was used. To simulate the flow conditions in the part of a boundary layer nearest the wall, a Couette flow velocity distribution and ambient temperature were prescribed at the inflow boundary. On the upper boundary, corresponding to the end of this linear part of the boundary layer, the velocity and ambient temperature were also prescribed. On the bottom boundary, two types of wall boundary conditions were considered: a highly conducting wall with prescribed ambient temperature (Section 4.2) and an insulating wall with Neumann boundary conditions (Section 4.3). The computational domain with corresponding boundary conditions can be seen in Fig. 7.

The Reynolds numbers, based on the cylinder diameter, considered in this investigation were very low, namely in the range 0.001–0.1. These are typical values for HWA near-wall measurements. Following the domain size rule for accurate Nu results, established in the course of the simulation of cylinders in free stream (Lange, 1997; Lange et al., 1998), the distance from the cylinder to the domain boundary should be 7500 times the cylinder diameter D for the lowest value of Re computed. However, a slightly larger error due to the domain size was admitted in this case and the domain boundary was placed at least 2000 diameters from the cylinder in each direction, with the obvious exception of the wall.

Wall distances Y_0/D between 10 and 300 were considered in the present study, where Y_0 is the distance from the center of the cylinder to the wall. The locally refined grid had a similar resolution around the cylinder as in the free stream computations (Section 3.3). As an example, the grid of the third multigrid level for the case of $Y_0/D = 100$ and a detailed view of the core region are shown in Fig. 8. The computations were performed on the fifth multigrid level with about 10^5 grid points.

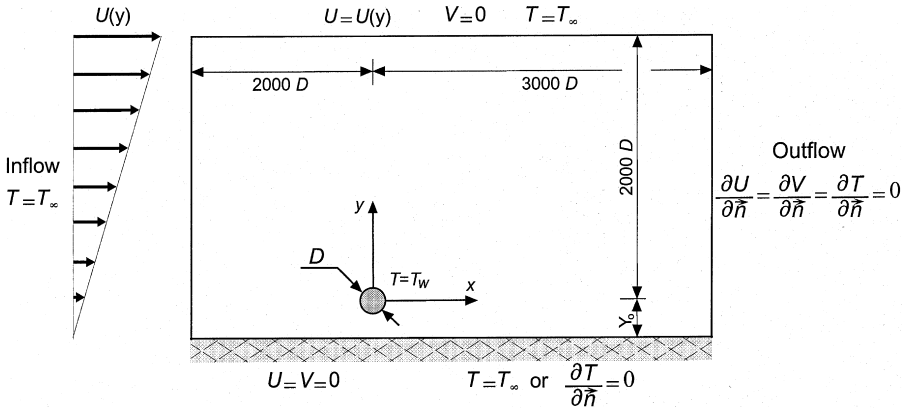

Fig. 7. Computational domain and boundary conditions for computations of flow around a heated cylinder in the vicinity of a wall.

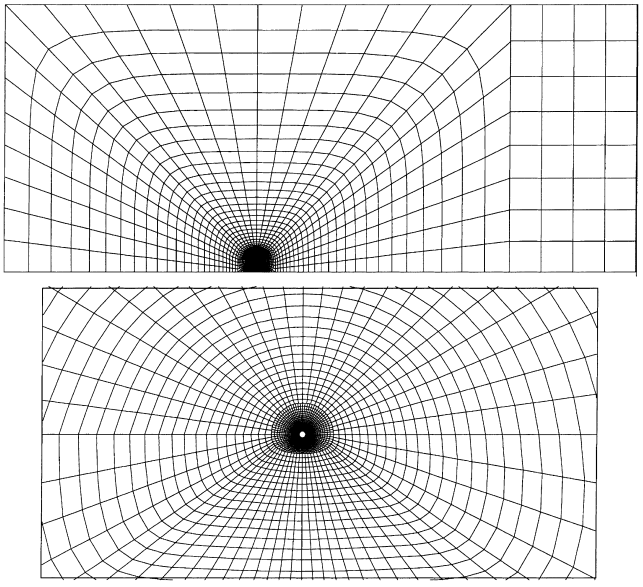

Fig. 8. Computational grid ($Y_0/D = 100$) and zoom of the locally refined region (both at the third of a total of five multigrid levels).

For each value of Y_0/D, several inflow velocity gradients were applied. The friction velocity $U_{\mathscr{F}}$, based on the conditions at inflow, varied between 0.006 and 0.1. The resulting range of nondimensional wall distances covered by the computations was $0.2 \leqslant Y^+ \leqslant 3.4$.

The fluid considered was air at an inflow (ambient) temperature of $T_\infty = 20°C$. The cylinder temperature T_w was successively set to 21°C, 50°C and 100°C, corresponding to temperature loadings [3] of $\mathscr{T} = 1.003, 1.1$ and 1.27, respectively. In the first case, the fluid properties were assumed to be constant, whereas at the larger values of $\mathscr{T}$ variable fluid properties were employed. In general, the CDS discretization was used for the computation of the convective terms. However, for the larger values of $U_{\mathscr{F}}$ the UDS discretization had to be employed to stabilize the computation, because of the large velocities occurring at the upper boundary.

[3] The temperature loading $\mathscr{T}$ should not be confused with $\mathscr{T}_w$, the molecular momentum transport term at the wall.

4.2. Predictions for highly conducting walls

In the case of a wall consisting of a heat-conducting material, the temperature gradient in the neighborhood of the cylinder is strongly increased, owing to the proximity of the wall. The additional heat transferred to the wall is the dominant cause of deviations in the HWA measurements. This was recognized by previous investigators, as described by Bruun (1995). This perception was also the justification for the neglect of any flow field distortion in the computations of Bhatia et al. (1982).

An example of the resulting temperature distribution due to the presence of a highly conducting wall is shown in Fig. 9. The additional heat loss at the cylinder surface, caused by the large heat flux transferred through the wall, is reflected by an increase in the mean Nu value at the cylinder.

The excess in the value of Nu, compared with the free stream flow, decreases with increasing local velocity for a given cylinder position Y_0/D. The local velocity U_0, i.e. the inflow velocity at the wire height Y_0, is the value to be obtained after correction of the HWA measurement data. An increase in the local velocity means also an increase in the velocity gradient at the wall and, consequently, in $U_{\mathscr{F}}$. For a given local velocity U_0, the deviation of Nu from the free stream value decreases also with increasing wall distance Y_0. These effects are demonstrated in Fig. 10 for the case of a temperature loading $\mathscr{T} = 1.27$, where the local velocity U_0 is represented by Re_∞, the Reynolds number formed with U_0, the cylinder diameter D and the kinematic viscosity at ambient temperature ν_∞.

In order to obtain a useful correction for HWA data in near-wall regions, the deviation of Nu has to be transformed into a velocity difference. If the HWA probe is calibrated at

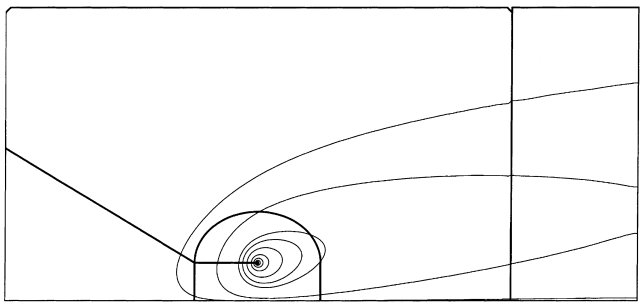

Fig. 9. Block boundaries and contours of temperature in the case of highly conducting wall ($Y_0/D = 300, \mathscr{T} = 1.27$ and $Y^+ = 1.7$ at wire position).

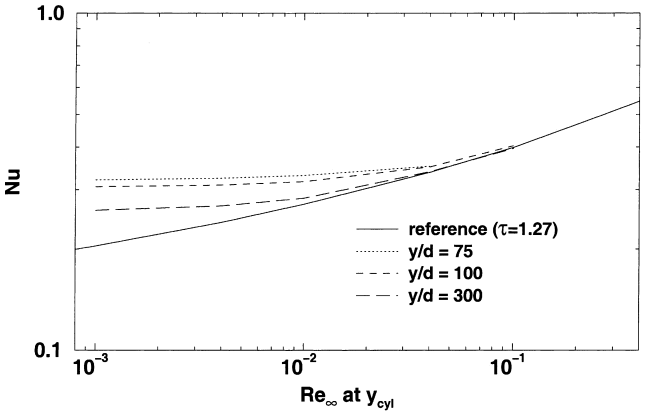

Fig. 10. Variation of Nu and Re_∞ at the cylinder height for different wire positions, compared with the reference Nu curve for free flow ($\mathscr{T} = 1.27$ and conducting wall).

free stream conditions, the apparent velocity in the wall vicinity U_{meas} is obtained by converting the measured Nusselt number Nu_{meas} into a Reynolds number Re_{meas} using the reference Nu curve established by calibration. In the present computations, the apparent velocity U_{meas} was determined in a similar way. By means of the computed Nusselt number Nu_{meas} and the reference Nu curves for $\mathscr{T} = 1.003$, 1.1 and 1.27 of Section 3.3, it was possible to obtain the apparent velocity U_{meas} that would be measured by an HWA probe. The actual local velocity U_0 was given by the boundary conditions.

Following almost all previous investigations on the subject, the resulting velocity differences were normalized to the friction velocity, resulting in values of ΔU^+, defined in Eq. (4). Finally, these values were plotted against the nondimensional wall distance Y^+ (defined in Eq. (2), using v_∞) with the aim of obtaining a single, universal curve for the velocity correction.

The curves for ΔU^+, resulting from the present computations are shown in Fig. 11. For comparison, several experimental curves and the numerical results of Bhatia et al. (1982) are also plotted. The interpolating curves from the experimental results of Oka and Kostić (1972) and Hebbar (1980) were extracted from a graphic by Bhatia et al. (1982). We recall that their raw data showed large scatter at both ends of the curves. From the results of Krishnamoorthy et al. (1985), only two particular cases were plotted, namely the two limiting values of temperature loadings measured with a hot-wire of diameter 5 μm, the same as the presently computed cylinder.

The corrections computed in the present study are clearly below the values obtained by Oka and Kostić (1972) and by Hebbar (1980). However, the calculated corrections show good agreement with the more recent results of Krishnamoorthy et al. (1985). Moreover, the present results also show a dependence on the temperature loading $\mathscr{T}$, confirming the findings of Krishnamoorthy et al. (1985). The good agreement of the computed corrections with data obtained by experiments on turbulent flows refutes the assertion of Wills (1962) that laminar flow corrections would tend to be twice as large as in the case of turbulent flows.

The agreement of the present results with the estimations of Bhatia et al. (1982) is poor. The assumption of no interference between the wall and the velocity field distortion caused by the cylinder was certainly not the main reason for the discrepancy. This interference plays a minor role in the Nu deviations, as will be shown in the next section. The principal error source in their results is presumably the critical conversion of computed Nu values into apparent velocities U_{meas}. Since the Nusselt curve is very flat in the region of low Re numbers, small errors in this transformation process are amplified in the resulting correction values. No information was given on how their calculated Nu results were converted into velocity corrections for HWA measurements.

The representation of velocity corrections by means of ΔU^+ has some disadvantages. First, the curve is not bounded at the lower end of the Y^+ range. Furthermore, ΔU^+ gives no idea of the relative dimension of the correction, compared with the apparent velocity measured. With the aim of obtaining a bounded function to fit the estimated corrections, a new representation is proposed. Instead of ΔU^+, the actual local velocity U_0 normalized to the apparent velocity U_{meas} is plotted against Y^+. The new correction, defined as

$$C_U = \frac{U_0}{U_{meas}} \tag{14}$$

constitutes a factor to be simply multiplied by the measured velocity U_{meas} in order to obtain the actual local velocity U_0.

The values of C_U obtained from the present computations for different temperature loadings are shown in Fig. 12 together with recent experimental results. The data of Hebbar (1980) and Krishnamoorthy et al. (1985) were transformed from ΔU^+ to C_U using the fact that $U^+ = Y^+$. The results are bounded at both ends and reveal immediately the fraction of correct information included in HWA data from near-wall regions. As the distance from the wall increases, the correction factor C_U tends to unity. On the other hand, at very close distances from the wall just a small portion of the measured HWA signal corresponds to the actual velocity information.

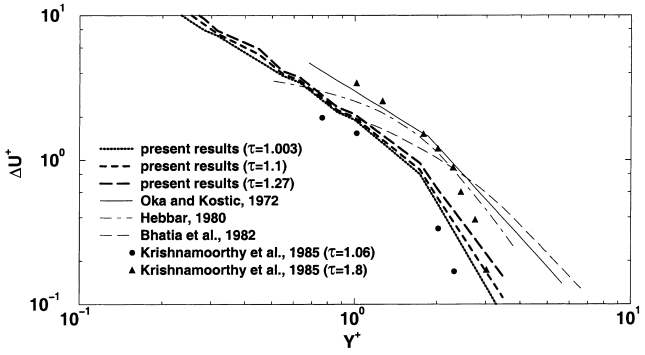

Fig. 11. Computed correction of ΔU^+ compared to experimental and numerical results from the literature in the case of a highly conducting wall.

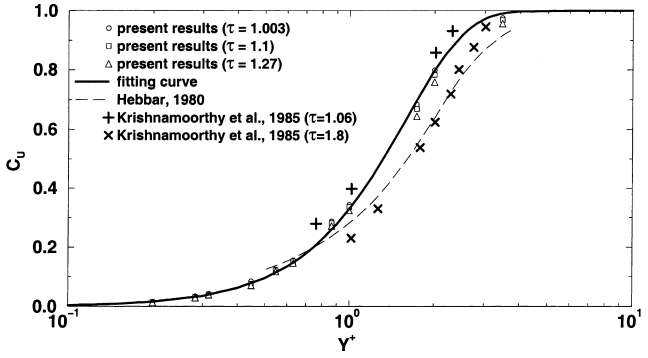

Fig. 12. Numerical and experimental values of the velocity correction factor C_U for different temperature loadings in the case of a highly conducting wall. The fitting curve corresponds to Eq. (15).

Another positive aspect of this representation is a reduction in the dependence on the temperature loading of the present results, as can be verified in Fig. 12.

The calculated values of the new correction factor C_U can be fitted for all temperature loadings considered with a good approximation by a relatively simple equation

$$C_U = 1.0 - \exp(-0.4Y^{+^2}). \tag{15}$$

The curve resulting from Eq. (15) is also shown in Fig. 12. Eq. (15) implies that less than 5% of an HWA signal would correspond to actual velocity measurements at a small distance of $Y^+ = 0.35$ from the wall. Based on the same equation, almost no correction (about 0.1%) to the measured velocity would be needed if the wire is more than $Y^+ = 4$ away from the wall. This is in agreement with the experimental results of Krishnamoorthy et al. (1985).

The new correction factor C_U together with Eq. (15) is expected to provide a better basis for further investigations on this subject, which should include a verification of the influence of the cylinder diameter, for example. In Section 4.3, a new insight into the physical problem is shown by means of the flow around a cylinder in the vicinity of an insulating wall.

4.3. Predictions for insulating walls

The temperature distribution of the flow problem investigated previously was characterized by the dominant effect of the heat loss through the highly conducting wall. In the case of a perfectly insulating wall material, no heat is extracted from the flow by the wall. In contrast, even the diffusive heat flux perpendicular to the main flow that would occur in a free stream is suppressed. This suppression causes an accumulation of heat between the cylinder and the wall, reducing the temperature gradient in this region. This effect can be easily recognized on the contours of the temperature in Fig. 13. The decrease on the temperature gradient at the cylinder surface causes a reduction in the measured Nusselt number and, hence, in the apparent velocity determined by an HWA probe.

An open question remaining from the investigations in the previous section is the role of the flow field interaction between the cylinder and the wall in the measured Nu deviations. This question will now be addressed. In addition to the important influence on the temperature distribution, a strong distortion of the flow field is also caused by the presence of the wall. By means of isolines of the velocity components (not shown here), it is possible to verify this effect. As a consequence of the flow contraction between the cylinder and the wall, the velocity gradient at the cylinder surface is increased, which brings about a small increase in the heat flux transferred by convection. However, the small Peclet numbers ($\mathrm{Pe} = \mathrm{Re}\,\mathrm{Pr}$) that characterize this kind of flow reflect precisely the minor role played by the convective heat transfer, compared with the heat transferred by conduction. This is the reason why the type of wall material plays the most important role in the determination of the velocity correction factors for the near-wall region.

The computed velocity corrections for the vicinity of a perfectly insulating wall are plotted in Fig. 14. The correction factor C_U, defined in the previous section (Eq. (14)), is again used to represent the correction needed for the measured velocity values. In this case the factor C_U is bounded between unity, for larger distances from the wall, and 1.36, at very small wall distances. Note that again just a very small influence of the temperature loading can be verified by the results in Fig. 14. The correction values calculated for the largest nondimensional wall distance $Y^+ = 3.46$ were obviously underestimated. In spite of this, they were plotted to show the clear tendency of the correction factors C_U towards unity.

An equation fitting the obtained correction values for the case of an insulating wall is given by

$$C_U = 1.0 + 0.363\,\exp(-0.22Y^{+^{2.5}}). \tag{16}$$

The correction curve corresponding to Eq. (16) is also shown in Fig. 14.

Contrary to the present conclusions, experimental investigations of the velocity correction needed in the case of nonconducting wall materials showed an increase in the measured velocity for $Y^+ \lesssim 2$, as described by Bruun (1995). These corrections were often interpreted as a consequence of the flow field interaction between wall and cylinder. The present results have shown that this interpretation is incorrect.

The apparent contradiction between experiments with nonconducting wall materials and the present numerical results is easily understood, if the values of the thermal conductivity k of air and common "insulating" materials are compared. Whereas air has a thermal conductivity $k \approx 0.026$ W/m K at ambient temperature, for plywood $k \approx 0.1$ W/m K and for Plexiglas $k \approx 0.2$ W/m K, i.e. 4–8 times the conductivity of air. Hence in comparison with air, these wall materials cannot be considered as nonconducting.

The comparison of the thermal conductivities makes it clear that experiments with "nonconducting" (i.e. less conducting) wall materials are to be considered as a combination of the two extreme cases presented. This means that, because of the lower conductivity of the wall, the heat-loss effect through the wall is not as dominant as in the case of a highly conducting material, such as a metal. In the ideal case of a wall with a similar thermal conductivity to the fluid, only the small effect of the flow contraction would influence the HWA near-wall measurements.

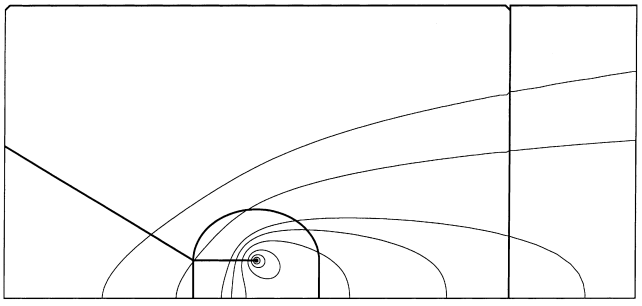

Fig. 13. Block boundaries and contours of the temperature in the case of an insulating wall ($Y_0/D = 300$, $\mathscr{T} = 1.27$ and $Y^+ = 1.7$ at wire position).

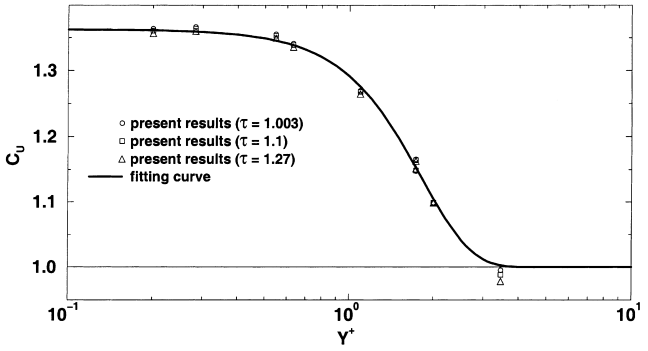

Fig. 14. Velocity correction factor C_U for different temperature loadings in the case of an insulating wall. The fitting curve corresponds to Eq. (16).

In view of these observations, further investigations on this subject should include the thermal conductivity of the wall as a parameter, since its influence on the correction factor C_U is expected to surpass by far the influence of other parameters, such as $\mathscr{T}$ or D.

5. Conclusions

By means of highly accurate computations for the two-dimensional laminar flow around a heated circular cylinder, the problem of HWA probes in the vicinity of rigid walls was addressed. The investigations were based on a very efficient finite volume code employing multigrid and local grid refinement techniques. In order to verify the numerical method, extensive and detailed predictions were performed for the flow and heat transfer around a two-dimensional cylinder under free stream conditions over the wide Re range 10^{-4} to 10^{2}. In the computations free convection effects were neglected. It can be argued by order of magnitude considerations that free convection effects are the same in the case of the wire being operated in free flows, i.e. away from the wall, and for being located close to a wall. Hence, taking the free convection term out of the equations for both the free flow computations and the computations close to a wall will not affect the final conclusions presented in this paper.

First, the behavior of the drag coefficient C_D and the Nusselt number Nu with Re was studied in detail for the case of a small temperature loading ($\mathscr{T} = 1.003$), when the fluid properties may be treated as constant. Good agreement was found in comparison with available experimental data and with analytical and numerical solutions in the range of their validity. The study was completed with the investigation of the influence of the temperature-dependent fluid properties on the flow and heat transfer. The temperature loading was varied between 1.003 and 1.5 and the resultant effect on the Nusselt number was analyzed. Applying the correction factor of Collis and Williams (1959) and consistently calculating Re and Nu at the film temperature, all computational results can be concentrated on a single curve.

After these verification predictions, the influence of the presence of a rigid wall in the vicinity of the cylinder was investigated which resembles the flow situation typically occurring in hot-wire anemometric measurements. For two limiting cases, namely a highly conducting and an insulating wall, it was possible to estimate the velocity correction needed by HWA measurement data. The computed results for the case of a highly conducting wall agree well with available experimental data. For the sake of convenience, a new form of velocity correction was suggested. The proposed correction factor C_U has the advantage of being bounded between 0 and 1 for the case of a highly conducting wall. Moreover, it transmits readily the relative magnitude of the influence of the wall on the measured apparent velocity and shows less dependence on the temperature loading of the hot-wire. The velocity field interference between the wall and the hot-wire was found to be less relevant to the deviation of Nu in near-wall regions than the interference by heat conduction, even in the case of an insulating wall, owing to the small Peclet numbers involved. This observation contrasts with the common opinion derived from previous experimental investigations.

The results for the case of an insulating wall were unexpected. Instead of larger apparent velocities, smaller values were observed. The corresponding correction factor C_U resulted in values between unity and the upper limit of 1.36. This contradicted previous experimental results. A detailed analysis of the numerical solution revealed new aspects of this complex flow situation. The accumulation of heat between the cylinder and the wall was found to be responsible for the unexpected effect. The apparent contradiction with experimental results was explained by the fact that common "nonconducting" wall materials actually have thermal conductivities much larger (4–8 times) than that of air. Therefore, these materials cannot be considered strictly as "nonconducting". They actually reflect a combination of the extreme cases calculated. In conclusion, the present work resulted in a better insight into this key problem of the HWA measurement technique. In order to improve further the correction of HWA measurements in the near-wall region, a more detailed study on the specific influence of the thermal conductivities of wall materials will be the subject of future investigations.

Acknowledgements

This work was supported by a fellowship from the German Academic Exchange Program (DAAD) to C.F. Lange and by a research grant from the Bavarian Consortium for High Performance Scientific Computing (FORTWIHR), which are gratefully acknowledged.

References

Aihara, Y., Kassoy, D.R., Libby, P.A., 1967. Heat transfer from circular cylinders at low Reynolds numbers II. Experimental results and comparison with theory. Phys. Fluids 10 (5), 947–952.

Barcus, M., Perić M., Scheuerer, G., 1988. A control volume based full multigrid procedure for the prediction of two-dimensional, laminar, incompressible flows. In: Deville, M. (Ed.), Notes on Numerical Fluid Mechanics, vol. 20, Braunschweig, Vieweg, pp. 9–16.

Barkley, D., Henderson, R.D., 1996. Three-dimensional Floquet stability analysis of the wake of a circular cylinder. J. Fluid Mech. 322, 215–241.

Bhatia, J.C., Durst, F., Jovanovic, J., 1982. Corrections of hot-wire anemometer measurements near walls. J. Fluid Mech. 122, 411–431.

Bruun, H.H. 1995. Hot-Wire Anemometry. Oxford University Press, Oxford.

Cole, J., Roshko, A., 1954. Heat transfer from wires at Reynolds numbers in the Oseen range. Proc. Heat Transfer and Fluid Mech. Inst. 6, 357–384. University of California, Berkeley, CA.

Collis, D.C., Williams, M.J., 1959. Two-dimensional convection from heated wires at low Reynolds numbers. J. Fluid Mech. 6, 357–384.

Dauchy, C., Dušek, J., Fraunié, P., 1997. Primary and secondary instabilities in the wake of a cylinder with free ends. J. Fluid Mech. 332, 295–339.

Demirdžić, I., Perić, M., 1990. Finite volume method for prediction of fluid flow in arbitrary shaped domains with moving boundaries. Int. J. Num. Methods Fluids 10, 771–790.

Dennis, S.C.R., Hudson, J.D., Smith, N., 1968. Steady laminar forced convection from a circular cylinder at low Reynolds numbers. Phys. Fluids 11 (5), 933–940.

Douglas, W.J.M., Churchill, S.W., 1956. Recalculation of data for convective heat transfer between gases and single cylinders with large temperature differences. Chem. Eng. Prog. 52 (18), 23–28.

Durst, F., Schäfer, M., 1996. A parallel blockstructured multigrid method for the prediction of incompressible flows. Int. J. Num. Meth. Fluids 22, 549–565.

Durst, F., Schäfer, M., Schreck, E., 1993. Parallelization of efficient numerical methods for flows in complex geometries. In: Hirschel, E.H. (Ed.), Flow Simulation with High-Performance Computers I: DFG Priority Research Programme Results 1989–1992, Vieweg, Braunschweig, pp. 79–92.

Dušek, J., Le Gal, P., Fraunié, P., 1994. A numerical and theoretical study of the first Hopf bifurcation in a cylinder wake. J. Fluid Mech. 264, 59–80.

Fand, R.M., Keswani, K.K., 1972. A continuous correlation equation for heat transfer from cylinders to air in crossflow for Reynolds numbers from 10^{-2} to 2×10^5. J. Heat Mass Transfer 15, 559–562.

Fand, R.M., Keswani, K.K., 1973. Recalculation of Hilpert's constants. J. Heat Transfer, Trans. ASME 95, 224–226.

Finn, R.K., 1953. Determination of the drag on a cylinder at low Reynolds numbers. J. Appl. Phys. 24 (6), 771–773.

Gersten, K., Herwig, H., 1984. Impuls- und Wämenübertragung bei variablen Stoffwerten für die laminare Plattenströmung. Wärme-Stoffübertragung 18, 25–35.

Hatanaka, K., Kawahara, M., 1995. A numerical study of vortex shedding around a heated/cooled circular cylinder by the three-step Taylor–Galerkin method. Int. J. Num. Methods Fluids 21, 857–867.

Hatton, A.P., James, D.D., Swire, H.W., 1970. Combined forced and natural convection with low-speed air flow over horizontal cylinders. J. Fluid Mech. 42 (1), 17–31.

Hebbar, K.S., 1980. Wall proximity corrections for hot-wire readings in turbulent flows. DISA Information 25, 15–16.

Henderson, R.D., Barkley, D., 1996. Secondary instability in the wake of a circular cylinder. Phys. Fluids 8 (6), 1683–1685.

Herwig, H., 1984. Näherungsweise Berücksichtigung des Einflusses variabler Stoffwerte bei der Berechnung ebener laminarer Grenzschichtströmungen um zylindrische Körper. Forsch. G. Ing. 50, 47–57.

Herwig, H., Wickern, G., 1986. The effect of variable properties on laminar boundary layer flow. Wärme-Stoffübertragung 20, 47–57.

Hieber, C.A., Gebhart, B., 1968. Low Reynolds number heat transfer from a circular cylinder. J. Fluid Mech. 32 (1), 21–28.

Hilpert, R., 1933. Wärmeabgabe von geheizten Drähten und Rohren im Luftstrom. Forsch. G. Ing. 4 (5), 215–224.

Hirota, I., Miyakoda, K., 1965. Numerical solution of Kármán vortex street behind a circular cylinder. J. Met. Soc. Japan 43 (1), 30–41.

Ho, C.J., Wu, M.S., Jou, J.B., 1990. Analysis of buoyancy-aided convection heat transfer from a horizontal cylinder in a vertical duct at low Reynolds number. Wärme-Stoffübertragung 25, 337–343.

Huner, B., Hussey, R.G., 1977. Cylinder drag at low Reynolds number. Phys. Fluids 20 (8), 1211–1218.

Ingham, D.B., 1968. Note on the numerical solution for unsteady viscous flow past a circular cylinder. J. Fluid Mech. 31 (4), 815–818.

Jayaweera, K.O.L.F., Mason, B.J., 1965. The behavior of freely falling cylinders and cones in a viscous fluid. J. Fluid. Mech. 22 (4), 709–720.

Kaplun, S., 1957. Low Reynolds number flow past a circular cylinder. J. Math. Mech. 6 (5), 595–603.

Karniadakis, G.E., Triantafyllou, G.S., 1992. Three-dimensional dynamics and transition to turbulence in the wake of bluff objects. J. Fluid Mech. 238, 1–30.

Kassoy, D.R., 1967. Heat transfer from circular cylinders at low Reynolds numbers. I. Theory for variable property flow. Phys. Fluids 10 (5), 938–946.

Kawaguti, M., 1953. Numerical solution of the Navier–Stokes equations for the flow around a circular cylinder at Reynolds number 40. J. Phys. Soc. Japan 8 (6), 747–757.

Kawaguti, M., Jain, P., 1966. Numerical study of a viscous fluid flow past a circular cylinder. J. Phys. Soc. Japan 21 (10), 2055–2062.

Keller, H.B, Takami, H., 1966. Numerical studies of steady viscous flow about cylinders. In: Greenspan, D. (Ed.), Numerical Solutions of Nonlinear Differential Equations, Wiley, New York, pp. 115–140.

Keller, J.B., Ward, M.J., 1996. Asymptotics beyond all orders for a low Reynolds number flow. J. Eng. Math. 30, 253–265.

Khosla, P.K., Rubin, S.G., 1974. A diagonally dominant second-order accurate implicit scheme. Comput. Fluids 2, 207–209.

King, L.V., 1914. On the convection of heat from small cylinders in a stream of fluid: determination of the convection constants of small platinum wires with applications to hot-wire anemometry. Phil. Trans. R. Soc. London A 214, 373–432.

Krishnamoorthy, L.V., Wood, D.H., Antonia, R.A., Chambers, H.J., 1985. Effect of wire diameter and overheat ratio near a conducting wall. Exp. Fluid 3 (3), 121–127.

Lamb, H., 1911. On the uniform motion of a sphere through a viscous fluid. Phil. Mag. 21, 112–121.

Lange, C.F., 1997. Numerical Predictions of Heat and Momentum Transfer from a Cylinder in Crossflow with Implications to Hot-Wire Anemometry. Ph.D. thesis, Institute of Fluid Mechanics, Friedrich–Alexander University of Erlangen-Nürnberg.

Lange, C.F., Durst, F., Breuer, M., 1998. Momentum and heat transfer from cylinders in laminar crossflow at $10^{-4} \leqslant \mathrm{Re} \leqslant 200$. Int. J. Heat Mass Transfer, to appear.

McAdams, W.H., 1954. Heat Transmission. McGraw-Hill Kogakusha, Tokyo, 3rd ed., 1954.

Merker, G.P., 1987. Konvektive Wärmeübertragung. Springer, Berlin.

Nakai, S., Okazaki, T., 1975. Heat transfer from a horizontal circular wire at small Reynolds and Grashof numbers - I: Pure convection. Int. J. Heat Mass Transfer 18, 387–396.

Nishioka, M., Sato, H., 1974. Measurements of velocity distributions in the wake of a circular cylinder at low Reynolds number. J. Fluid Mech. 65, 97–112.

Noack, B.R., Eckelmann, H., 1994. A global stability analysis of the steady and periodic cylinder wake. J. Fluid Mech. 270, 297–330.

Nusselt, W., 1915. Das Grundgesetz des Wärmeüberganges. Gesund.-Ing. 38 (42), 477–482.

Oka, S., Kostić, Z., 1972. Influence of wall proximity on hot-wire velocity measurements. DISA Information 13, 29–33.

Oseen, C.W., 1910. Über die Stokes'sche Formel und über eine verwandte Aufgabe in der Hydrodynamik. Art. Mat. Astron. Fys. 6(29).

Perić, M., 1985. A Finite Volume Method for the Prediction of Three-Dimensional Fluid Flow in Complex Ducts. Ph.D. thesis, Imperial College, London.

Perić, M., 1990. Analysis of pressure–velocity coupling on nonorthogonal grids. Num. Heat Transfer. Part B 17, 63–82.

Prandtl, L., Wieselsberger, C., Betz, A., 1923. Ergebnisse der aerodynamischen Versuchsanstalt zu Göttingen, vol. II, R. Oldenburg Verlag, Munich.

Proudman, I., Pearson, J.R., 1957. Expansions at small Reynolds numbers for the flow past a sphere and a circular cylinder. J. Fluid. Mech. 2, 237–262.

Schäfer, M., Schreck, E., Wechsler, K., 1993. An efficient parallel solution technique for the incompressible Navier–Stokes equations. In: Hebeker, F.-K., Rannacher, R., Wittum, G. (Eds.), Numerical Methods for the Navier–Stokes Equations, vol. 47 of Notes on Numerical Fluid Mechanics, Vieweg, Braunschweig, pp. 228–238.

Schlichting, H., Gersten, K., 1997. Grenzschicht-Theorie. Springer, Berlin, 9th ed.

Schmidt, E., Wenner, K., 1941. Wärmeabgabe über den Umfang eines angeblasenen geheizten Zylinders. Forsch. G. Ing. 12 (2), 65–73.

Stokes, G.G., 1851. On the effect of the internal friction of fluids on the motion of pendulums. Trans. Camb. Phil. Soc. 9 (Part 2), 8–106.

Sucker, D., Brauer, H., 1975. Fluiddynamik bei quer angeströmten Zylindern. Wärme-Stoffübertragung 8, 149–158.

Sucker, D., Brauer, H., 1976. Stationärer Stoff-und Wärmeübergang an stationär quer angeströmten Zylindern. Wärme-Stoffübertragung 9, 1–12.

Sundén, B., 1983. Influence of buoyancy forces and thermal conductivity on flow field and heat transfer of circular cylinder at small Reynolds number. Int. J. Heat Mass Transfer 26 (9), 1329.

Sundén, B., 1992. Viscous heating in forced convective heat transfer across a circular cylinder at low Reynolds number. Int. J. Num. Methods Eng. 35, 729–736.

Tamada, K., Miura, H., Miyagi, T., 1983. Low-Reynolds-number flow past a cylindrical body. J. Fluid Mech. 132, 445–455.

Thom, A., 1933. The flow past circular cylinders at low speed. Proc. Roy. Soc. Lond. A 141, 651–669.

Thoman, D.C., Szewczyk, A.A., 1969. Time-dependent viscous flow over a circular cylinder. Phys. Fluids 12 (Suppl. 2), 76–86.

Tomotika, S., Aoi, T., 1951. An expansion formula for the drag on a circular cylinder moving through a viscous fluid at small Reynolds numbers. Quart. J. Mech. Appl. Math. 4 (4), 401–405.

Tritton, D.J., 1959. Experiments on the flow past a circular cylinder at low Reynolds numbers. J. Fluid Mech. 6, 547–567.

Verein Deutscher Ingenieure, 1991. VDI-Wärmeatlas. VDI, Düsseldorf, 6th ed.

Wehle, F., Brandt, F., 1982. Einfluss der Temperaturabhängigkeit der Stoffwerte auf den Wärmeübergang an der laminar überströmten ebenen Platte. Wärme-Stoffübertragung 16, 129–136.

Wieselsberger, C., 1921. Neuere Feststellungen über die Gesetze des Flüssigkeits- und Luftwiderstandes. Phys. Z. 22 (11), 321–328.

Williamson, C.H.K., 1996. Vortex dynamics in the cylinder wake. Annu. Rev. Fluid Mech. 28, 477–539.

Wills, J.A.B., 1962. The correction of hot-wire readings for proximity to a solid boundary. J. Fluid Mech. 12, 388–396.

Wood, W.W., 1968. Calculation for anemometry with fine hot wires. J. Fluid Mech. 32 (1), 9–19.

Žukauskas, A., Žiugžda, J., 1985. Heat Transfer of a Cylinder in Crossflow. Hemisphere/Springer, Washington, D.C.